Physical modeling and numerical analyses of vibro-driven piles with evaluation of their applicability for offshore wind turbine support structures

Aligi Foglia
Fraunhofer Institute for Wind Energy and Energy System Technology (IWES), Germany, aligi.foglia@iwes.fraunhofer.de

Martin Kohlmeier and Maik Wefer
Fraunhofer Institute for Wind Energy and Energy System Technology (IWES), Germany

ABSTRACT

Vibro-driven piles can potentially become cost-reducing alternatives to standard impact-driven piles for offshore wind turbine support structures. If these foundations are to be used to support jacket sub-structures, their bearing behaviour in tension has to be explored. In a novel geotechnical testing facility two large-scale vibro-driven piles for jacket sub-structures have been axially tested in tension. In this contribution the experimental tests are thoroughly described and the test results are presented. The applicability of standard CPT methods in predicting the tensile bearing capacity of the piles is evaluated against the experimental results. In addition, a simplified 2D axisymmetric numerical model is adopted to interpret the initial stiffness of the pile-soil interaction. As also pointed out in previous studies the ultimate resistance of the piles turns out to be significantly smaller than the CPT method prediction. Furthermore, as expected, set-up and pre-loading effects are seen to be beneficial to the tensile bearing behaviour of the pile.

Keywords: vibro-driven piles, offshore foundations, large-scale tests.

1 INTRODUCTION

Offshore wind energy is a necessary part of the present and future European energy mix. As reported in Valpy (2014) and Fichtner (2013) the levelised cost of energy (LCOE) decreases for large turbine rated power. Relevant offshore wind potential is still untapped in water depths exceeding 45-50 m. In such water depths, large wind converters will be most likely supported by jacket structures founded on piled foundations. Most offshore piles are installed with impact-driven piles, whose noise must be reduced with expensive techniques in order to limit the damage on sea mammals, as required by the German authority BSH (2013). In sandy soils a viable alternative to impact-driven piles are vibratory-driven piles. Instead of applying a number of strikes on the pile head to penetrate the foundation into the soil, vibratory drivers grip the pile head and apply quick sequences of downward and upward motions to the pile in order to reach the required embedded length. As also presented in Matlok (2015) vibro-driven piles offer, with respect to impact-driven piles, the following advantages:

- No noise mitigation system required when installing
- Faster installation
- No fatigue induced by impact-driving (potential saving in steel for piles)

These advantages might bring savings in the range of 5% to 10% of foundation fabrication and installation costs (Matlok, 2015).

Piles supporting jacket structures (diameter between 1.5 m and 4 m) are mainly subjected to vertical loading in tension and compression. The axial capacity of a piled foundation under compressive loads has two contributions: the base resistance and the shaft resistance. In sandy soils the shaft resistance is assessed based on the CPT cone resistance whereas in clayey soils it is quantified as a function of the undrained shear strength. The ultimate base resistance is defined with an allowable vertical displacement criterion and is calculated by summing the contributions of external pile shaft resistance, base resistance and either soil plug or internal pile shaft resistance. Obviously, in case of tensile loading, the base resistance has no influence on the pile capacity. As emphasized in recent publications (Igoe et al., 2013; Achmus et al., 2015) the tensile loading of piles supporting multipod sub-structures for offshore wind turbines are very important and can in some cases be the design driver.

This paper describes a large-scale experimental campaign investigating vibro-driven piles subjected to tensile loading. The experimental results are then interpreted to estimate the economical viability of this relative novel technology for offshore wind.

1.1 Specific aims of the study

Research on vibro-driven piles has so far focused on installation analysis (Viking, 2002), onshore piles subjected to compressive loading (Lammertz, 2008; Borel, 2006) and offshore piles subjected to overturning moment (LeBlanc et al., 2013). With respect to piles predominantly subjected to axial loads, it is not yet clear whether the economic advantages mentioned above would be able to outweigh a potential increase in pile dimension due to limitations in bearing capacity. In other words, the cost reduction previously outlined can have an impact on the project economics only if vibro-driven piles have similar capacity to the traditionally adopted impact-driven piles. Thus, the first specific aim of this study is to understand whether the ultimate tensile capacity predicted with the standard CPT-methods gives comparable results to the large scale test data presented in this contribution. Another crucial analysis for the complete understanding of the soil–structure interaction concerns the initial axial stiffness of the geotechnical system. The second specific aim of the contribution focuses on this aspect for the axially loaded pile. A 2D axisymmetric finite element model with a simplified pile is validated in terms of initial stiffness against the test results.

The test campaign and the data interpretation was carried out within the European Union-funded project INNWIND.EU which aims at investigating innovative key components of wind turbines with rated capacities between 10 MW and 20 MW.

2 LARGE-SCALE TEST DESCRIPTION

The experimental campaign has been executed by Fraunhofer IWES in the new Test Centre for Support Structures of the Leibniz University in Hannover. Among others, the research facility accommodates a foundation test pit which consists of reinforced concrete walls containing 9 m wide, 14 m long and 10 m deep volume of sand. Abutment walls on one side of the pit and various displaceable steel frames, allow for testing offshore wind foundations subjected to different loading conditions. A picture of the empty sand pit is shown in Figure 1.

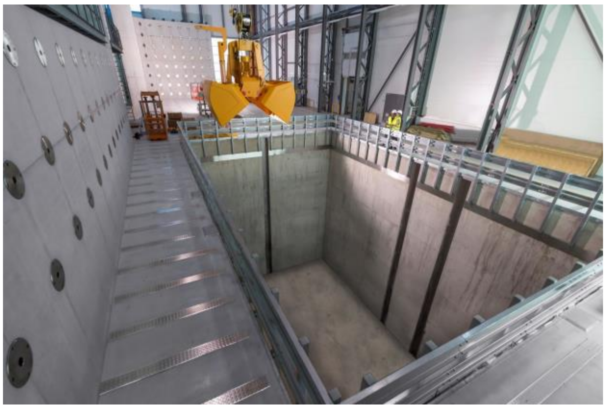

Figure 1 Sand pit of Test Centre before sand filling. Dimensions: 9 m x 14 m x 10 m.

Table 1 Properties of Rohsand 3152.

Property	Symbol	Unit	Value
Maximum void ratio	e_{max}	-	0.83

Minimum void ratio	e_{min}	-	0.44
Specific gravity	G_s	-	2.65
Coefficient of uniformity	C_u	-	1.97
Coefficient of curvature	C_c	-	0.98
Grain diameter to 60% passing material	d_{60}	mm	0.407

The testing material used is uniformly graded siliceous sand called Rohsand 3152, which was provided by the company Schlingmeier Quarzsand GmbH & Co. KG based in Schwülper, Germany. The fundamental properties of the sand are presented Table 1.

2.1 Preparation of the sand sample

High-quality geotechnical experiments require systematic sand preparation procedures to obtain:

- Uniform samples
- Repeatable samples
- A designated degree of compaction

In the present experimental campaign the aim was to create medium dense to dense sand condition (relative density, *Dr* between 55% and 70%), which is representative for sandy deposits of the North Sea. In order to achieve these, the sand was poured into the pit and compacted in subsequent layers. The compaction was performed with direction plate compactors. The sand layers had a thickness of about 30 cm before the compaction which reduced to 25 cm after the compaction. The first three meters from the bottom were prepared with an initial thickness of 50 cm.

2.2 Property of the piles

Two identical piles (Pile 1 and Pile 2), made of steel S355, were installed and subsequently tested. The dimensions of the piles are diameter, D = 0.508 m, length, L = 7,5 m (embedded length L_e = 6 m) and wall thickness, t = 6.3 mm. In order to be able to install and test the pile, a flange to which adaptors for installation and tensile test can be adjusted was appropriately designed. The scale of the model is between 1:4 and 1:8 depending on the prototype considered.

2.3 Assessment of the soil properties

Three soil investigation techniques were adopted to assess the sand status after the soil preparation procedures:

- Soil core samples (CS)
- Dynamic probe light (DPL)
- Cone penetration test (CPT)

The sand pit area was equally divided into six sub-areas. The soil samples were carefully taken with a cylindrical soil sampler (diameter 10 cm, length 12 cm) from every sub-area after each compacted layer. The relative density (*Dr*), averaged over the six sub-areas is plotted against depth in Figure 2. The relative density ranges between 0.55 and 0.72 with an average value of 0.61. It is worth to mention that the relative density calculated with soil core needs neither empirical parameter nor sophisticated empirical equation to be evaluated, and is therefore highly reliable. Thus, the curve referring to soil core samples depicted in Figure 2 is utilized further in this section as mean of comparison to validate the empirical

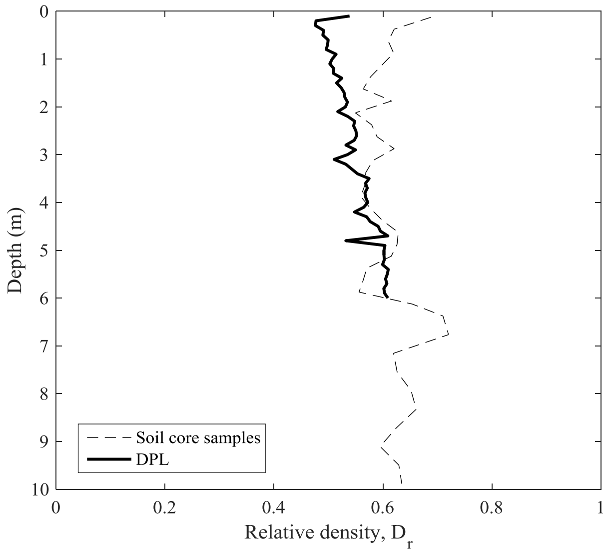

Figure 2 Average relative density calculated over the cross area according to CS and DPL.

methods necessary to evaluate *Dr* with DPL and CPT. Information on the sand pit uniformity can be acquired by calculating the coefficient of variation (COV) of the relative density data of the six samples for each compacted layer.

The COV shows very moderate values (between 0.02 and 0.12), revealing uniform relative density across the sand pit and small variation with depth.

To gain more insight into uniformity and to predict parameters of the soil, dynamic probing tests (DPLs) and cone penetration tests (CPTs) were performed. More importantly, CPTs were necessary to be able to use CPT-based methods for axially loaded piles (API, 2011). In Figure 3 a plan view of the sand pit with indication of the inspection points (IPs) referring to CPTs and the position of the piles installed, are shown. DPLs and CPTs were performed closed to each other (0.5 m distance) on purpose, to gain a correlation law between the two methods of investigation. DPLs were conducted down until 6 m whereas CPTs down until 9.4 m.

In Figure 2 the average relative density over the cross area on the base of DPLs data, calculated according to EN (1997), is plotted against depth. The soil core samples curve shows good match with the DPLs curve only from a depth of about 3 m. This corroborates the well-known fact that cone resistance is dramatically influenced by the very low confining stresses characteristic of sand at shallow depths.

In Figure 4 the CPT profiles of all the IPs are depicted. The cone tip resistance (*qc*), between 1m and 7m of depth, presents values ranging from 5 to 23 MPa. Approximately the last three meter (roughly between 7m and 9.4m), *qc* decreases. This is most probably due to the different preparation system used in that specific region of the sample. It should be noticed though that this inconsistency will not negatively affect the test results. Indeed, the tensile bearing capacity of piles does not involve soil below the pile but almost exclusively soil adjacent to the pile shaft.

A peek up to 35 MPa in tip resistance can be seen at a depth of 6.2 m. This occurred in position IP3 where most probably the cone came across a stone.

When interpreting CPT data of real sites, it is common to use relationships correlating CPT tip resistance and relative density of the sand (see Baldi et al., 1986; Clausen et al., 200: DIN, 2002; Puech et al., 2002). These approaches are also used here in an attempt to understand which method is the most suitable given the experimental condition described above. The estimation of *Dr* based on the average value of *qc* (across the area of the pit) is plotted against the depth according to four different approaches in Figure 5.

It must be mentioned that these approaches were thought for real scale data and much larger depths. Their applicability in moderate depth (namely 10 m) is not obvious.

By observing Figure 5, it is immediately apparent that the four approaches give very different *Dr* values, particularly within the first two to three meters. This is not surprising, and can be ascribed to the influence of low confining pressure on the cone resistance (see Puech et al., 2002). However, the four approaches seem to be more consistent to each other with increasing depth, as it should be expected. The method Puech et al. (2002) is clearly the most suitable for the sand pit, at least for the first two to three meters. This is a reassuring observation since this particular method was formulated ad hoc for shallow penetration CPTs.

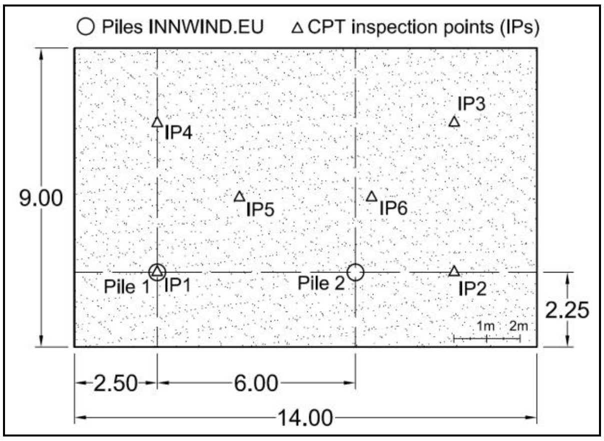

Figure 3 Plan view of the sand pit with indication of the inspection points (IPs) for CPT.

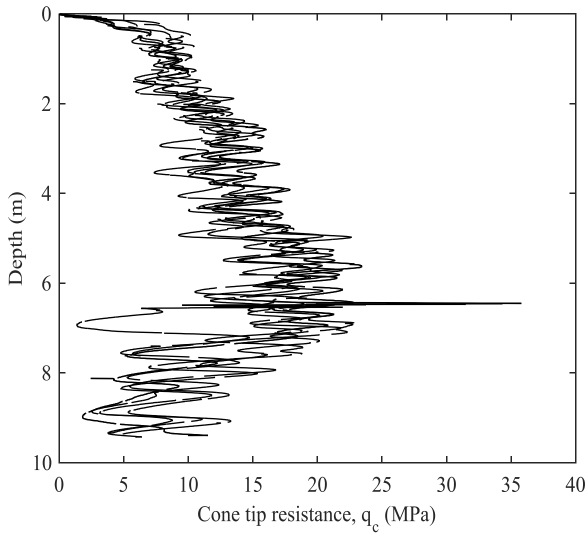

Figure 4 CPT profiles of all the inspection points.

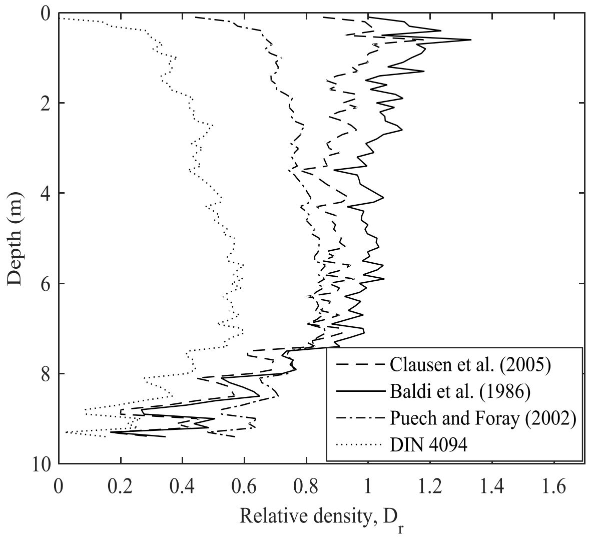

Figure 5 Interpretation of CPT data. Relative density according to four different methods.

From three to seven meter down, the method overestimates *Dr* by 15%. The methods Clausen et al. (2005) and Baldi et al. (1986) overestimate the *Dr* quite remarkably at shallow depth for then being more consistent at six to seven meters depth. The method DIN (2002) underestimates *Dr*, particularly in the first meters. Down at six to seven meters depth DIN (2002) seems to give very appropriate values of *Dr*.

2.4 Test phases

In this section, all the steps overtaken before and during the tensile tests are described. As already mentioned before in the paper, the two piles installed are named Pile 1 and Pile 2. Pile 1 was installed first and was subjected

Figure 6 Picture of the test setup just before the tensile loading test of Pile 2.

to pre-loading before being tested under tensile loading. Pile 2 was installed thereafter and was only subjected to tensile loading until failure. A picture of the test setup with both piles indicated is shown in Figure 6. During the tensile loading tests the piles were monitored with load cell of the actuator, displacement transducer of the actuator and external displacement transducer. The actuator used for the test has a capacity of 500 kN. The external displacement transducer was installed in order to enable a system-independent measurement of the pile uplift during tensile loading. The external transducer and the internal transducers of the actuator are connected to an analyzer unit which in turn broadcasts the signal to the computer unit where the data are stored with a sampling frequency of 100 Hz.

The installation of the piles was carried through by an external firm specialized in deep foundations. Pile 1 was installed on February 5th, 2015. Pile 2 was installed on August 6th, 2015. The installation was performed by an excavator. The vibratory hammer was connected to the arm of the excavator which in turn grabbed the adaptor placed at pile head.

The pile penetrated the sand with a velocity of approximately 0.1 m/s. Pile 2 was installed with a vibrator type ICE 8RFB, which has a frequency of 14 Hz. Pile 1 was installed with a vibrator type Müller MS-5 HFBV, which has a frequency of 45 Hz.

As already mentioned, Pile 1 was subjected to relevant pre-loading before being axially tested in tension. The pre-load applied in this phase consisted of cyclic horizontal quasi-static load with different amplitudes. Additionally, a 0.9 m deep scour was artificially created. In this manner the influence of set-up effect (about 200 days after the installation), scour, installation frequency and pre-loading were to be explored. Given the scale of the system it was not possible to apply the different effects to more than one foundation. As a result of that the implications of these affecting variables could not be possibly decoupled. However, it is well known that the set-up effect is generally beneficial to the bearing behavior of piles as also recently reported by Lehane et al. (2005). Further, scouring phenomena are doubtlessly negative for the bearing behavior. The question arises as whether pre-loading produces beneficial of detrimental effects on the pile shaft capacity. This query could unfortunately not be answered within this experimental campaign.

A very robust steel structure formed by two vertical columns and supporting a horizontal beam was employed to offer the necessary counterweight to the system (see Figure 6). The 500 kN hydraulic cylinder (actuator) was connected to the beam on one side and, by means of a steel adapter plate, to the flange of the pile. A picture of the setup for Pile 2 is illustrated in Figure 7 where displacement transducer, pile and actuator are indicated. The test was performed in a displacement-controlled manner. To make sure that no pore pressure building up could possibly occur during the tensile loading test, a very low displacement rate (0.01 mm/s) designated. This displacement rate was also confirmed by the external displacement transducer.

Before the tensile loading test a difference of 82 cm between soil on the inside and on the outside of the pile was measured (Plug length Ratio of 86%). After the test the difference between soil level in and soil level out the pile was measured again with the same result. This proves that the behavior of the pile was substantially fully plugged during the tensile loading test.

3 PRESENTATION AND INTERPRETATION OF THE EXPERIMENTAL DATA

A magnified view of the curves for the first 10 cm vertical displacement is depicted in Figure 8. The entire load-displacement curve for both tests is shown in Figure 9 together with the CPT methods predictions. In the initial 0.4 mm of vertical displacement the curves appear to be identical. After this similar initial stiffness branch, it is evident that the two piles show essentially different behaviours. Pile 2 keeps hardening for the whole test showing no peak capacity. Pile 1 shows a distinct peak resistance in correspondence to a displacement of about 6 mm (≈1/100 *D*). The ultimate capacity of Pile 1 is 177 kN and was taken as the peak load reached at circa 6 mm of displacement. The ultimate capacity of Pile 2 is 115 kN and was taken according to the well-established 1/10 *D* criterion. Even disregarding the negative presence of the scour and the higher installation frequency, set-up and pre-loading effects seem to benefit the tensile ultimate resistance by 53%.

Figure 7 Pile 2 before the tensile loading test.

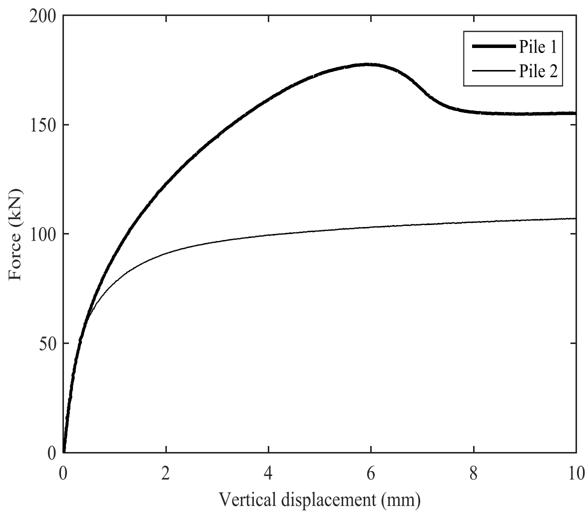

Figure 8 Load-displacement curve of both piles. Initial 10 mm of vertical displacement.

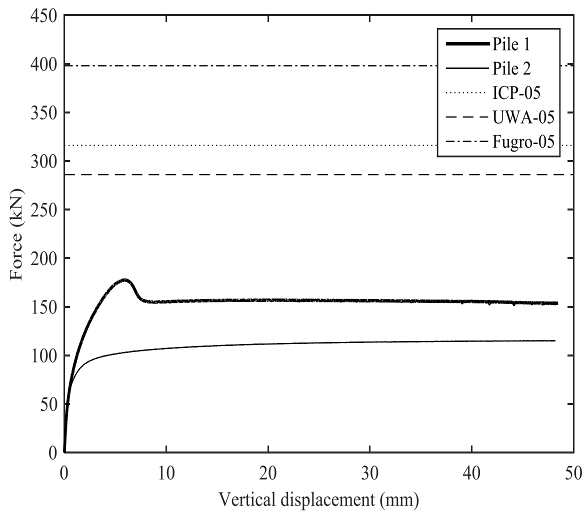

Figure 9 Experimental data in comparison to CPT methods prediction.

3.1 Interpretation of the ultimate resistance by means of the CPT methods

The applied CPT methods for axially loaded piles are the empirical formulas developed by the four different research groups: Imperial College (ICP), University of Western Australia (UWA), Norwegian Geotechnical Institute (NGI) and Fugro. They relate CPT measurements with the axial capacity in tension and in compression of purely axially loaded piles. A comprehensive and comparative review of the methods is given in Lehane et al. (2005). The methods are also included in the offshore foundation standard API (2011) with the names ICP-05, UWA-05, Fugro-05 and NGI-05. This nomenclature will be retained in this paper as well. The calculations concerning CPT-methods presented in this report were performed with the IGtHPile software developed by the Institute of Geotechnical Engineering (IGtH), Leibniz Universität Hannover, Germany.

Usually, the input data for CPT methods are an average of raw CPT data calculated over a specified distance step. The distance step chosen was 0.5 m. Table 2 gives an overview of the CPT based method predictions in comparison with the tensile capacity tests. It is immediately apparent that the experimental tensile capacity is overpredicted by all the CPT methods. The experimental result of Pile 1 is in proportion between 27% and 61% of the CPT methods prediction. The same information is visually presented in Figure 9 where the NGI-05 method is omitted to allow appropriate representation of the experimental data. In accordance to Achmus and Müller (2010) the most suitable approaches for open-ended piles in tension are the ICP-05 and the UWA-05. This seems to be confirmed also by the test data of this study, which show the smaller deviation for the ICP-05 and UWA-05 methods. The quite relevant discrepancy between CPT-based estimation and experimental result is to be ascribed to the installation method used. As already mentioned, CPT-based approaches were calibrated with impact-driven and pressed piles data. A recalibration of CPT-based method on the base of an extensive vibro-driven piles campaign tests is therefore suggested. The tests so far performed, corroborate the previous finding of other researchers (Borel et al., 2006); the shaft resistance of vibro-driven piles is smaller than that of impact-driven piles.

Table 2 Summary of ultimate capacity prediction in comparison to the experimental data.

Method	Ultimate Capacity (kN)	Pile 2/ CPT meth. Prediction	Pile 1/ CPT meth. Prediction
ICP-05	316	0.36	0.56
UWA-05	286	0.40	0.61
Fugro-05	398	0.29	0.44
NGI-05	648	0.18	0.27

3.2 *Interpretation of the initial stiffness by means of a numerical model*

The numerical model was created with the finite element program ABAQUS (2014). The 2D-axisymmetric model is formed by axisymmetric elements of the type CAX4. The laboratory physical situation is recreated in the model. In the numerical model the distance between the pile axis and the retaining wall (boundary condition) was taken as the minimum distance present in the laboratory (5 pile diameters). The discretization of the model is shown in Figure 10. A very fine mesh was created in the vicinity of the pile. The pile was modelled with a linear-elastic material with Young's Modulus E_{steel} = 2.1·10^5 MPa and Poisson's ratio of ν = 0.3. For the soil the Mohr-Coulomb failure criterion is adopted. The stiffness modulus of the sand, *E*, was derived by means of oedometric tests (11 MPa) and CPTs (17 MPa).

The soil is fully saturated except for the most superficial 20 cm. Despite of that, only one soil strata with effective unit weight, γ' = 10.15 kN/m^3, was considered. A Poisson's ratio of 0.27 was used. The friction angle, ϕ', was chosen as the critical friction angle characteristic for the sand with that particular compaction state. A value of ϕ' = 33º was chosen on the base of direct shear tests previously conducted on the sand.

The hypothesis of pile wished in place was made. The coefficient of lateral earth pressure at rest was calculated as $K_0 = 1 - \phi'$.

The model was constructed so that the pile is a solid section with equivalent weight and stiffness modulus to the real system (pile plus saturated soil inside). As a result of that, only the self-weight of a plugged pile plus the external shaft resistance contribute to the tensile resistance. For modelling the pile-soil contact an elasto-plastic contact interaction was considered. The friction coefficient was calculated with the well-known equation $\mu = \tan(\delta) = \tan(2/3\phi')$. The displacement at which full frictional stress mobilization occurs (elastic slip) was set to 2 mm. The parameters used are listed in Table 3. The model was carefully checked by applying different loads to the pile in tension and compression and by calculating thereafter equilibrium between forces applied and resultant stresses. To enable the achievement of a clear plastic plateau at the end of the curves and also to simulate the physical experiment, the simulations were run displacement-controlled and thus by applying a particular displacement to the pile head. A considerable number of parameter studies was carried out in order to have a clear understanding of the model parameters. The model responded as expected to the parameter change. The displacement-force curves relative to three different *E* moduli are shown in Figure 11. As expected, the three curves present equal ultimate capacity and significantly different initial stiffness. The change in initial stiffness is consistent with the different values of the *E* modulus.

In Figure 12 the model prediction is plotted against the test curves. It can immediately be seen that the load-displacement behaviour of the model calculated with *E* = 17 MPa underestimate considerably the test curve. Indeed, the physical model shows a much higher initial stiffness. In order to have reasonable match with the experimental curve the *E* modulus of the sand has to be increased to 120 MPa. This value of *E* is undoubtedly out of the normally used range.

This indicates that substantial changes in the model are required in order to capture the experimental behaviour with realistic parameters.

Table 3 Parameters used for sand and contact model.

Property	Symbol	Unit	Value
Friction angle	ϕ'	º	33
Soil-pile interface angle	δ	º	22
Effective unit weight	γ'	kN/m^3	10.15
Poisson's ratio	ν	-	0.27
Dilation angle	ψ	º	10
Young's moduli	*E*	MPa	17, 120

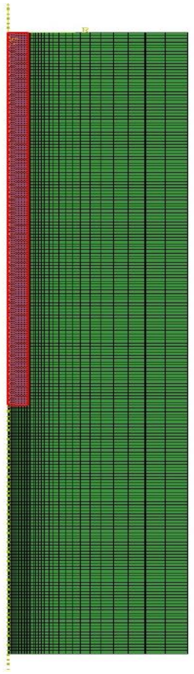

Figure 10 Discretization of the 2D - axisymmetric model. Pile emphasized in red colour.

It is furthermore deemed that by modelling appropriately the soil-steel interface behaviour, the entire response (initial stiffness and ultimate resistance) of a pile under tensile loading can be well simulated.

4 FINAL REMARKS

Two vibro-driven piles have been tested in large-scale to explore their economic feasibility for jacket-supported offshore wind turbines. The following conclusions can be drawn:

- Even disregarding the negative effects of higher installation frequency and scouring, it was found that set-up phenomena and pre-loading are beneficial to the ultimate tensile capacity by 53%. A crucial finding is also that the initial stiffness of the pile was not influenced by them. The number of the large-scale tests was very limited and the specific influence of each and every effect could not yet be decoupled.
- The CPT methods seem to overestimate considerably the experimentally derived ultimate capacity. However, in order to estimate more accurately the discrepancy in ultimate capacity between impact- and vibro-driven piles, the same piles should be installed with impact hammer and tested.
- A simple axisymmetric numerical model could not capture the initial stiffness behaviour with realistic values of *E*. A more sophisticated contact model should be used to gain better simulations with more realistic soil parameters.

ACKNOWLEDGEMENT

The experimental campaign and the data post-processing presented in this contribution

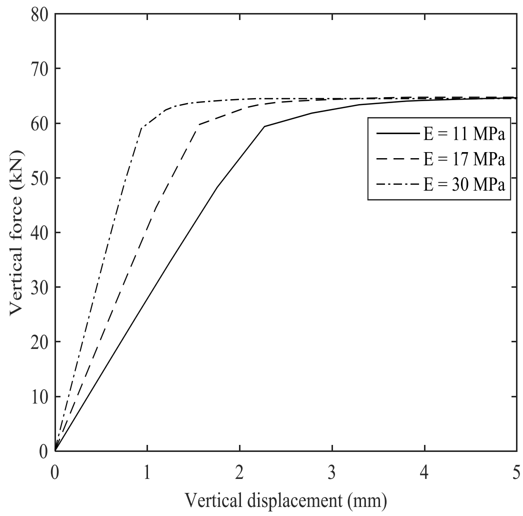

Figure 11 Load-displacement curves of the numerical model with three different E moduli.

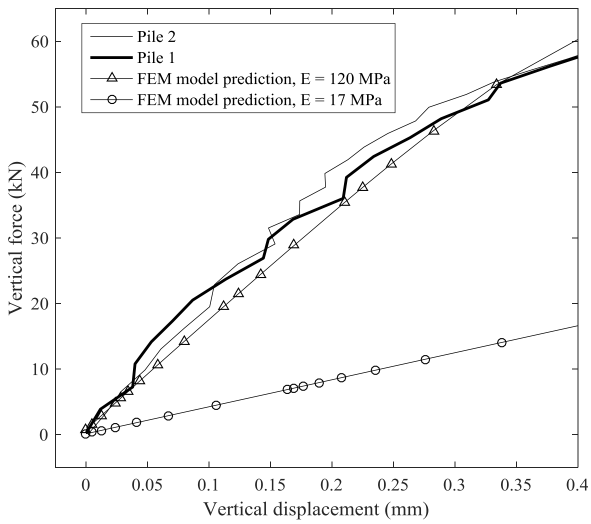

Figure 12 Comparison of load-displacement curves of numerical model and experimental test.

have been carried out as part of the INNWIND.EU project (7th Framework

Programme FP7-ENERGY-2012-1-2STAGE under grant agreement No. 308974).

5 REFERENCES

ABAQUS (2014). 6.14 User’s Manual. Simulia, Providence, USA.

Achmus, M., Müller, M. (2010). Evaluation of pile capacity approaches with respect to piles for wind energy foundations in the North Sea. 2nd International Symposium on Frontiers in Offshore Geotechnics, 8-10 November 2010, University of Western Australia, Perth.

Achmus, M., Lemke, K., Abdel-Rahman, K., Kuo, Y.-S. (2015). Numerical approach for the derivation of interaction diagrams for piles under cyclic axial loading. Proceedings of the Twenty-fifth International Ocean and Polar Engineering Conference.

API (2011). ISO 19901-4:2003 (Modified), Petroleum and natural gas industries-Specific requirements for offshore structures, Part 4-Geotechnical and Foundation Design Considerations.

Baldi, G., Bellotti, R., Ghionna, V., Jamiolkowski, M., Pasqualini, E. (1986). Interpretation of CPT's and CPTU's. 2nd Part: drained penetration on sands. Proc., 4th Int. Geotech. Seminar: Field Instrumentation and In Situ Measurements, Nanyang Technol. Univ., Singapore, 143–162.

Borel, S., Bustamante, M., Rocher-Lacoste, F. (2006). The comparative bearing capacity of vibratory and impact driven piles. International symposium on vibratory pile driving and deep soil vibratory compaction.

BSH (2013). Offshore Wind Farms Measuring Specification for the Quantitative Determination of the Effectiveness of Noise Control Systems. Bundesamt für Seeschifffahrt und Hydrographie.

Clausen, C. J. F., Aas, P. M., Karlsrud, K. (2005). Bearing capacity of driven piles in sand, the NGI approach. – Proc., 1st Int. Symp. on Frontiers in Offshore Geotechnics, Balkema, Perth, Australia, 677–681.

DNV (2010). Offshore standard DNV-OS-J101: Design of offshore wind turbine structures. Technical report DNV-OS-J101, Det Norske Veritas.

DIN, (2002). Baugrund; Felduntersuchungen. 4094 Teil 1: Drucksondierungen. – Beuth, Berlin.

EN (2007). 1997-2: Eurocode 7: Geotechnical design - Part 2: Ground investigation and testing [Authority: The European Union Per Regulation 305/2011, Directive 98/34/EC,Directive 2004/18/EC].

Fichtner (2013). Cost Reduction Potentials of Offshore Wind Power in Germany.

Igoe, D., Gavin, K., O’Kelly, B. (2013). An investigation into the use of push-in pile foundations by the offshore wind sector. International Journal of Environmental Studies.

Lammertz, P. (2008). Ermittlung der Tragfähigkeit vibrierter Stahlrohrpfähle in nichtbinigem Boden. PhD thesis, Universität Duisburg-Essen.

LeBlanc, C., Liingaard, M.A., Shajarati, A., Kallehave D., Skov Gretlund J. (2013). Vibro-driving of monopiles-experience from Anholt Offshore Wind Farm, Offshore EWEA, Frankfurt.

Lehane, B.M., Schneider, J.A. and Xu, X. (2005). A review of design methods for offshore driven piles in siliceous sand. UWA Report GEO 05358.

Puech, A., Foray, P. (2002). Refined model for interpreting shallow penetration CPTs in sands. – Offshore technology conference (OTC 14275). Houston, Texas.

Valpy, B., English, P., Martínez, A., Simonot, E. (2014). Future renewable energy costs: offshore wind. BVG Associates and KIC InnoEnergy.

Matlock, B.G.W.M. (2015). Comparison of the lateral bearing capacities of hammered and vibrated piles. 5th Internationa Conference Offshore Foundations, Bremen.

Viking, K. (2002). Vibro-driveability – A field study of vibratory driven sheet piles in non-cohesive soils. PhD thesis, Royal Institute of Technology Stockholm.